

1 **Green dehydrogenation of dimethylamine borane catalyzed by cheaply copper(0)**  
2 **nanocatalysts without any stabilizer at nearly room temperature**

3 **Ali ÖZDEMİR and Sibel DUMAN\***

4 *Department of Chemistry, Bingol University, Bingol, 12000, Turkey*

5 \*Correspondence: sduman@bingol.edu.tr

6 ORCIDs:

7 First AUTHOR: <https://orcid.org/0000-0002-9357-7209>

8 Second AUTHOR: <https://orcid.org/0000-0003-1517-9800>

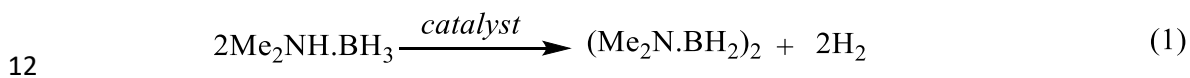
9 **Abstract:** In this work, the findings of the work on the green dehydrogenation behavior  
10 of molten dimethylamine borane (DMAB) catalyzed by the precatalyst copper(II)  
11 acetylacetonate ( $\text{Cu}(\text{acac})_2$ ) in solvent-free medium (green) at near room temperature  
12 (nRT,  $30.0 \pm 0.1^\circ\text{C}$ ) were reported. Herein, a complete study has been presented which  
13 includes: (i) synthesis and catalytic activity of Cu(0) NCats in solvent-free medium, (ii)  
14 determination of activation energy for Cu(0) NCats catalyzed green dehydrogenation of  
15 DMAB, (iii) demonstration of catalytic lifetime of Cu(0) NCats, (iv) test of isolability  
16 and reusability of Cu(0) NCats, (v) poisoning experiments using carbon disulfide on a  
17 per-active-copper-atom basis, (vii) **characterization of Cu(0) NCats by UV-vis, XRD,**  
18 **XPS and TEM/HRTEM/TEM-EDX spectroscopies. In addition, ATR-FTIR and  $^{11}\text{B}$**   
19 **NMR techniques were use to characterize the cyclic aminoborane product obtained as a**  
20 **result of dehydrogenation of dimethylamine-borane.**

21 **Key words:** Copper, dimethylamine-borane, green dehydrogenation, heterogeneous  
22 catalysis, nanocatalysts.

23

## 1 1. Introduction

2 With the increasing demand for energy in recent years, scientists have started to show great  
3 interest in alternative energy sources. Accordingly, hydrogen stands out as a sustainable,  
4 renewable and clean energy source [1,2]. Hydrogen, which is a secondary energy source  
5 of the future is considered as the most important energy carrier [3,4,5]. However, the most  
6 important issue for hydrogen is the storage problem, which limits its applicability. In this  
7 context, amine-boranes with high hydrogen storage capacity remain promising [6,7,8].  
8 Dimethylamine borane (DMAB,  $(\text{CH}_3)_2\text{NH}\cdot\text{BH}_3$ ) as solid hydrogen storage agent occupies  
9 a special position among the amine-boranes because of its gravimetric hydrogen storage  
10 capacity (6.9%) and its excellent stability and environmental friendliness [9,10,11]. Also,  
11 DMAB releases one equivalent dihydrogen ( $\text{H}_2$ ) using a suitable nanocatalyst (Eq. 1).



13 There are several techniques to produce dihydrogen using DMAB which is one of  
14 the best solid materials for hydrogen storage [12]. Usually, dihydrogen is acquired by  
15 dehydrogenation of DMAB catalyzed by convenient metal nanocatalysts at high  
16 temperatures or in a solvent environment [13,14,15,16,17,18,19,20,21,22,23,24]. In the  
17 previously, we reported the effect of using oleylamine on copper(0) nanoparticles for the  
18 catalytic dehydrogenation of DMAB in solvent (5.0 mL toluene) and at relatively high  
19 temperature ( $50.0\pm 0.1^\circ\text{C}$ ) [25]. In this study, we provided a full transformation of DMAB  
20 ( $\text{Me}_2\text{NHBH}_3$ ) to cyclic aminoborane ( $[\text{Me}_2\text{NBH}_2]_2$ ) and obtained one equivalent  
21 dihydrogen with  $\text{TOF}_{\text{app}}$  (initial apparent turnover frequency) values of 158 and  $71 \text{ h}^{-1}$  for  
22 copper(0) nanoparticles with and without oleylamine, respectively [25]. More  
23 importantly, for the dehydrogenation of DMAB in the solution medium, the Arrhenius  
24 activation energies of copper(0) nanoparticles with and without oleylamine were

1 calculated as  $E_a = 19 \pm 2$  and  $88 \pm 2$  kJ mol<sup>-1</sup>, respectively, and these values were  
2 comparable to the others (Table 1, see later). Although copper nanoparticles with and  
3 without oleylamine used for the dehydrogenation of DMAB have high activity at  
4  $50.0 \pm 0.1^\circ\text{C}$ , the Cu(0) nanoparticles achieved by reduction of copper(II) acetylacetonate  
5 in this study do not require stabilizers and solvents, and the dihydrogen is released upon  
6 dehydrogenation of DMAB at a lower temperature (nRT,  $30.0 \pm 0.1^\circ\text{C}$ ). Nowadays, it is  
7 very important to perform economic studies, and with this study, four important economic  
8 advantages were obtained: (i) no solvents, (ii) no stabilizers (iii) no expensive metals, and  
9 (iv) no high temperatures. The results are qualitatively compared with the catalytic effects  
10 of copper catalysts reported previously (see later). However, our recent study has shown  
11 that there is efficient and effective dihydrogen release in the dehydrogenation of DMAB  
12 even at temperatures below nRT in solvent-free environments using catalysts such as  
13 nickel ( $25.0 \pm 0.1^\circ\text{C}$ ) [26] and ruthenium ( $35.0 \pm 0.1^\circ\text{C}$ ) [27]. The literature survey shows  
14 that although there are a few copper nanoparticles or complexes synthesized using amine-  
15 boranes in solvent environment or at high temperature, there are no reports of using  
16 copper metal as a catalyst for green (solvent-free) dehydrogenation of DMAB [28,29].  
17 As in previous studies, DMAB has two important roles as stabilizer and reducing agent  
18 in the synthesis of Cu(0) nanocatalysts (NCats) throughout the dehydrogenation reaction.  
19 Moreover, an experiment was carried out with the calculations of TOF (total frequency)  
20 and TON (turnover number) values to determine the catalytic lifetime of Cu (0) NCats.  
21 The result of this experiment showed that the Cu (0) NCats provided comparable TOF<sub>app</sub>  
22 ( $47.7 \text{ h}^{-1}$ ) and TON (456.5 at 50 h) values for green dehydrogenation of DMAB in nRT.  
23 Cu(0) NCats exhibited high activity and stability for the dehydrogenation reaction  
24 throughout the catalytic run thanks to the stabilizing property of molten DMAB and

1 maintained their initial activity at 81% even after the 5th run with full conversion in the  
2 green dehydrogenation of DMAB. Cu(0) NCats and by-products of DMAB formed after  
3 the dehydrogenation reaction were characterized by  $^{11}\text{B}$  NMR, UV-vis, ATR-FTIR,  
4 XRD, XPS and TEM/HRTEM/TEM-EDX techniques. The heterogeneity of Cu(0) NCats  
5 synthesized from the green dehydrogenation of DMAB was tested using 0.1 equiv of  
6 carbon disulfide per copper atom. In order to calculate the rate law and activation energy  
7 ( $E_a$ ), kinetic studies were performed throughout the green dehydrogenation of DMAB  
8 catalyzed by Cu(0) NCats depending on substrate amounts, catalyst amounts and  
9 temperature. Thus, it can be assumed that highly active Cu(0) NCats are a good option  
10 for the green dehydrogenation of DMAB at nRT and will make an important contribution  
11 to the literature.

12

13

14

15

16

17

18

19

20

21

22

23 **Table 1.** Comparison of catalytic activity, particle size and reusability catalysts reported plus  
24 activation energy of the catalytic dehydrocoupling of DMAB.

| (Pre)catalyst  | TOF<br>(h <sup>-1</sup> ) | Ea<br>(kJmol <sup>-1</sup> ) | Particle size<br>(nm) | Reusability<br>(Cycle)     | Ref.              |
|--|---------------------------|------------------------------|-----------------------|----------------------------|-------------------|
| Dimethylammonium<br>Hexanoate Stabilized<br>Rh(0) NCs                      | 60                        | 34                           | 1.9                   | <sup>a</sup> ND            | [14]              |
| OAm stabilized Ru(0)<br>NPs  | 137                       | 29                           | 1.8                   | 75% (5 <sup>th</sup> )     | [21]              |
| Pd NPs@Cu <sub>3</sub> (btc) <sub>2</sub>                                  | 75                        | 173.5                        | 4.3                   | 80% (5 <sup>th</sup> )     | [30]              |
| Ru NPs/ZIF-8   | 0.98                      | 42.5                         | 1.9                   | 85% (5 <sup>th</sup> )     | [31]              |
| <i>mer</i> -<br>[Ru(N <sub>2</sub> Me <sub>4</sub> ) <sub>3</sub> (acac)H] | 0.3                       | 85                           | <sup>a</sup> ND       | <sup>a</sup> ND            | [32]              |
| <sup>b</sup> Ni NPs  | <sup>c</sup> 21           | 42                           | 1.9                   | 63% (5 <sup>th</sup> )     | [26]              |
| <i>trans</i> -<br>[Ru(acac) <sub>2</sub> (OAm) <sub>2</sub> ]              | 77.8                      | 58                           | <sup>a</sup> ND       | <sup>a</sup> ND            | [33]              |
| Pt(0)/OA@CNT   | 44.36                     | 42.91                        | 3.2                   | >80% (4 <sup>th</sup> )    | [34]              |
| Pt(0)/DOA@CNT  | 57.32                     | 40.23                        | 3.4                   | >80% (4 <sup>th</sup> )    | [34]              |
| Ru(0)/APTS   | 55                        | 61                           | 1.7                   | 70% (6 <sup>th</sup> )     | [16]              |
| Copper(0) NPs  | 71                        | 88                           | <sup>a</sup> ND       | >54% (3 <sup>th</sup> )    | [25]              |
| OAm stabilized<br>copper(0) NPs  | 158                       | 19                           | 3.5                   | 74% (5 <sup>th</sup> )     | [25]              |
| <sup>b</sup> Ru@PVP NCs  | <sup>d</sup> 56           | 18                           | 12.9                  | 87% (5 <sup>th</sup> )     | [27]              |
| <sup>b</sup> Ru@PS-co-MA NCs   | <sup>d</sup> 29           | 45                           | 24.9                  | 63% (5 <sup>th</sup> )     | [27]              |
| <sup>b</sup> Ru@Al <sub>2</sub> O <sub>3</sub> NCs                         | <sup>d</sup> 51           | 25                           | 11.9                  | 80% (5 <sup>th</sup> )     | [27]              |
| <b><sup>b</sup>Cu(0) NCats</b>   | <b><sup>e</sup>47.7</b>   | <b>16.6</b>                  | <b>2.9</b>            | <b>81%(5<sup>th</sup>)</b> | <b>This study</b> |

1 <sup>a</sup>ND: not demonstrated. <sup>b</sup>These nanoclusters were synthesized during green dehydrocoupling of DMAB.

2 <sup>c</sup>This TOF value was obtained within 4 h. <sup>d</sup>These TOF values were obtained within 2 h. <sup>e</sup>This TOF value

3 was obtained after induction period within 50 h.

#### 4 **2. Experimental method**

## 1 **2.1. Materials**

2 Cu(acac)<sub>2</sub> (Copper(II) acetylacetonate, 97%), dimethylamine-borane complex (DMAB,  
3 Me<sub>2</sub>NHBH<sub>3</sub>, 97%), carbon disulfide (CS<sub>2</sub>, ≥99%), THF-d<sub>8</sub> and hexane (99%) were bought  
4 from Sigma-Aldrich<sup>®</sup>. Ethanol was bought from Merck<sup>®</sup>. Acetone was used to clean all  
5 glass materials and Teflon-coated magnetic stir bars. All materials were rinsed a few  
6 times with copious amounts of distilled water and then dried at high temperature (110°C)  
7 in the oven during the night.

## 8 **2.2. Characterization**

9 Prior to Transmission Electron Microscopy (TEM) analysis, nanocatalysts were washed  
10 by repeated centrifugation in 10 mL ethanol and redispersed by ultrasonication in 3x15  
11 mL hexane. TEM instrument (JEM-2010F (JEOL), 200 kV, 4.5 Å point resolution) was  
12 used to acquire TEM, HRTEM and TEM-EDX images of these prepared nanocatalysts.  
13 By withdrawing 0.5 mL aliquots of Cu(0) NCats dispersed in hexane, they were  
14 transferred to deposit on silicon oxide coated copper grids TEM using a disposable  
15 polyethylene pipette. These grids were immersed in the solution for five seconds and then  
16 the volatiles were evaporated under an inert gas atmosphere. Magnifications of the  
17 nanocatalysts were performed between 100 and 400 k. Assuming that the nanocatalysts  
18 were spherical, the diameters of the individual particles were calculated from the  
19 corresponding surface area. Size scattering was expressed as mean diameter ± standard  
20 deviation. <sup>11</sup>B NMR spectra belong to DMAB and side product of DMAB (near 0.01 mg)  
21 obtained from the reactor in THF-d<sub>8</sub> were recorded using Bruker Avance DPX 400 MHz  
22 spectrometer (128.15 MHz) and boron trifluoride etherate (BF<sub>3</sub>(C<sub>2</sub>H<sub>5</sub>)<sub>2</sub>O) was used as an  
23 external reference for them. Powder X-ray diffraction (XRD) patterns were recorded 2θ  
24 in the range of 5 to 90° using the Rigaku Ultima-IV diffractometer (CuKα, λ= 1.54051

1 Å, 40 kV, 55 mA) at 25°C (room temperature, RT). To describe the elemental surface  
2 composition and chemical bonding properties, the XPS spectrum was recorded with a  
3 Specs-Flex XPS photoelectron spectrometer using an Al-coated anode of toroidal quartz  
4 single crystal design. The transmission energy values can be continuously selected from  
5 a minimum of 1 eV to 400 eV. UV–visible spectra of precursor Cu(acac)<sub>2</sub> and Cu(0)  
6 NCats resolved in 20 µL hexane were recorded in the spectral range of 200-800 nm using  
7 a Shimadzu 1800 double beam spectrometer. The infrared spectra of DMAB and its by-  
8 products were recorded using a Perkin Elmer A 100 ATR/FTIR spectrometer.

### 9 **2.3. Common processes and detailed kinetic studies for the green dehydrogenation** 10 **of DMAB catalyzed by Cu(0) NCats**

11 To perform the green dehydrogenation of DMAB under nitrogen atmosphere, an  
12 experimental setup consisting of jacketed reactor (50 mL), Teflon-covered mixing bar,  
13 magnetic mixer (IKA®C-Mag HS7) and fixed temperature bath (Polyscience 12107-15  
14 water bath) was set up. All reactions for the dehydrogenation of DMAB catalyzed by  
15 Cu(0) NCats were carried out according to the standard Schlenk technique, used fixed  
16 amounts of molten DMAB and Cu(acac)<sub>2</sub> at nRT. The jacketed reactor was closed after  
17 addition of the calculated amounts of reactants, the temperature was fixed using  
18 thermostatic bath and at the same time the stirrer was rotated at 1000 rpm. This procedure  
19 was repeated for all reactions. **The data of pressure versus time of hydrogen release during**  
20 **the catalytic dehydrogenation reaction was calculated using Microsoft Office Excel 2010**  
21 **and Origin2016 and then converted into the equivalent and volume (mL) of hydrogen per**  
22 **mole DMAB.**

23 Kinetic studies of the dehydrogenation of DMAB catalyzed by Cu(0) NCats were  
24 performed in three groups depending on the amounts of DMAB and copper and

1 temperature. 1<sup>st</sup> group experiments were carried out as a function of catalyst amount,  
2 keeping the number of moles of DMAB fixed (2.0 mmol) and varying the number of  
3 moles of Cu(acac)<sub>2</sub> between 0.1-0.3 mmol at nRT. 2<sup>nd</sup> group experiments were performed  
4 as a function of substrate amount, mol Cu(acac)<sub>2</sub> was kept fixed (0.2 mmol) and mol  
5 DMAB was varied between 1.0-3.0 mmol at nRT. 3<sup>rd</sup> experiments were carried out as a  
6 function of temperature, moles of Cu(acac)<sub>2</sub> and DMAB were kept constant (0.2 and 2.0  
7 mmol) respectively, and the temperature was varied between 25-45°C. Arrhenius plot [35]  
8 and values of k<sub>obs</sub> (observed rate constant) obtained from the slopes of the linear sections  
9 of the dehydrogenation curves were used to calculate the activation energy (E<sub>a</sub>).

#### 10 **2.4. Determination of catalytic lifetime for green dehydrogenation of DMAB** 11 **catalyzed by Cu(0) NCats**

12 The value of the total turnover number (TON) was used to determine the lifetime of Cu(0)  
13 NCats throughout green dehydrogenation of DMAB. In order to determine lifetime of  
14 Cu(0) NCats during green dehydrogenation of DMAB, a new experiment was started with  
15 0.2 mmol Cu(acac)<sub>2</sub> and 2.0 mmol DMAB at nRT. When the expected hydrogen gas  
16 release was complete, more DMAB was re-added to the reaction medium and this process  
17 was continued in this manner until no more hydrogen gas release was monitored.

#### 18 **2.5. Heterogeneity test for Cu(0) NCats throughout green dehydrogenation of** 19 **DMAB**

20 Recent studies have clearly shown that CS<sub>2</sub> has high poisoning ability and is used in  
21 heterogeneity tests of metal nanoparticles because CS<sub>2</sub> adsorbs on the metal surface due  
22 to the reduced reaction medium [26]. Generally, a poisoning test is carried out as follows:  
23 In the dehydrogenation of 2.0 mmol molten DMAB in a solvent-free environment, 0.1  
24 equiv. of CS<sub>2</sub> per copper was added to in situ formed 0.2 mmol of Cu(0) NCats after the



1 50% conversion. By observing the rate of dihydrogen release after and before the addition  
2 of CS<sub>2</sub> (0.1 equiv. per copper) to the dehydrogenation reaction, the effect of the poison  
3 was followed and measured. The poisoning experiments were terminated when  
4 dihydrogen release was no longer monitored.

## 5 **2.6. Reusability, isolability and bottlability of Cu(0) NCats in green dehydrogenation** 6 **of DMAB**

7 After the dehydrogenation of DMAB (2.0 mmol) was completed in the presence of Cu(0)  
8 NCats achieved from the reducing precursor Cu(acac)<sub>2</sub> (0.2 mmol ) at nRT, the reaction  
9 was stopped. The reaction flask was then sealed and separated from a graduated glass  
10 tube. Finally, after releasing the hydrogen pressure, it was transferred to a new reaction  
11 flask under N<sub>2</sub> atmosphere. Using 20 mL of cold hexane, the solid mixture was  
12 precipitated under inert atmosphere and these suspended particles were separated by  
13 filtration. Then, the solid was washed with ethanol (3x20 mL), the isolated colloid was  
14 dried under vacuum and obtained as a black powder. This black powder was reused by  
15 adding DMAB again at nRT to determine its catalytic activity throughout the green  
16 dehydrogenation (five runs in total).

## 17 **3. Results and discussion**

### 18 **3.1. Achieving and identification of Cu(0) NCats in green dehydrogenation of DMAB**

19 As is well known, the dehydrogenation of DMAB does not proceed without a catalyst,  
20 whether it is a solvent or a solvent-free environment. Therefore, we first tested the  
21 Cu(acac)<sub>2</sub> salt, which we intended to use as a precursor catalyst, in the presence of various  
22 solvents for the dehydrogenation of DMAB at nRT. No formation of Cu(0) NCats and no  
23 manufacture of dihydrogen were observed with this precursor throughout the green  
24 dehydrogenation of DMAB in many solvents (THF, toluene, etc.) at nRT. By using cheap

1 metals such as copper for the green dehydrogenation of DMAB, it is clear that special  
2 conditions are required for the classical synthesis of a highly stable and active  
3 nanocatalyst, such as increasing the temperature or using a suitable stabilizer. This  
4 assumption was confirmed by our recent work, in which oleylamine was used as a  
5 stabilizer and highly active copper(0) nanoparticles were synthesized throughout the  
6 dehydrogenation of DMAB in toluene solution at a relatively higher reaction temperature  
7 ( $50.0 \pm 0.1^\circ\text{C}$ ) [25]. Moreover, this study, like our previous studies [26,27], supports that  
8 the best results for the synthesis of active and stable Cu(0) NCats are obtained from the  
9 dehydrogenation of DMAB under solvent-free (green) environmental conditions.  
10 Consequently, Cu(0) NCats that are active and stable even after several weeks of storage  
11 were synthesized in situ without stabilizer and solvent by using Cu(acac)<sub>2</sub> as a precursor  
12 throughout the dehydrogenation of DMAB at nRT. Moreover, these nanocatalysts and  
13 the dehydrogenation reaction products isolated after washing in ethanol were identified  
14 by <sup>11</sup>B NMR, UV-vis, ATR-FTIR, XRD, XPS and TEM/HRTEM/TEM-EDX  
15 techniques.

16 The catalytic activity of Cu(0) NCats throughout the catalytic green  
17 dehydrogenation of DMAB was measured using the standard Schlenk technique as  
18 described in the Experimental Section. First, a series of experiments were performed to  
19 determine the effect of the mol ratio of DMAB:Cu(0) NCats on the green  
20 dehydrogenation of the catalytic DMAB, and it was found that this ratio is about 10 to  
21 provide and monitor the full reduction from the Cu<sup>2+</sup> to the Cu<sup>0</sup> oxidation state. This ratio  
22 is the best-known to obtain high activity of cheap and non-noble metals such as copper  
23 for the catalytic green dehydrogenation of DMAB [25]. When the formation of Cu(0)  
24 NCats was completed (after ~45 min of induction period), dihydrogen release from the

1 green dehydrogenation of DMAB started and the hydrogen pressure was manually  
2 recorded from the water level in the graduated glass tube minute by minute (Figure 1).  
3 While no dihydrogen release was monitored throughout the induction period of about 45  
4 min required for reduction of  $\text{Cu}^{2+}$  to  $\text{Cu}^0$ , it was clearly observed that almost all of the  
5 dihydrogen (1.0 equiv) was rapidly removed within the first 45 min after catalyst  
6 formation (hence the total time of approximately 110 min after induction time). The plot  
7 of dihydrogen release versus time shows that the formation of  $\text{Cu}(0)$  NCats and the  
8 concomitant green dehydrogenation of DMAB occurred in a short time. Herein, it is  
9 clearly seen that  $\text{Cu}(0)$  NCats have high stability and activity in hydrogen production  
10 from green dehydrogenation of DMAB (Figure 1).

11 During the green dehydrogenation of DMAB, the formation and oxidation state  
12 of  $\text{Cu}(0)$  NCats were monitored by UV and XPS spectroscopies (Figure 2). The UV–  
13 visible spectra and color change (from blue to black) explain the rapid degradation of  
14  $\text{Cu}(\text{acac})_2$  ( $\text{Cu}^{2+}$ ) to copper nanocatalysts ( $\text{Cu}^0$ ) after a visible induction period of ~45 min  
15 during the dehydrogenation of DMAB. Figure 2a shows the UV-visible spectra of  
16 solutions containing  $\text{Cu}(\text{acac})_2$  in hexane before and after injection into the reaction solids  
17 mixture. Examination of the UV spectra reveals three absorption peaks at  $\lambda_{\text{max}} = 243$ ,  
18 323 and 563-803 nm for  $\text{Cu}(\text{acac})_2$ , which can be attributed to the charge transfer from  
19 metal to ligand (CTML),  $\pi$ - $\pi^*$  electron transition and d-d electron transition, respectively  
20 (Figure 2a) [36]. After the reduction of  $\text{Cu}^{2+}$  ions, these bands disappeared and a  
21 characteristic Mie exponential decay profile for copper nanocatalysts was observed,  
22 which is consistent with the literature [37].

23 High-resolution XPS analysis of  $\text{Cu}(0)$  NCats (Figure 2b) confirmed the presence  
24 of copper in agreement with TEM-EDX result. Figure 2b shows that this XPS spectrum

1 contains two prominent bands at 934.15 and 951.24 eV, assigned to Cu(0) 2p<sub>3/2</sub> and Cu(0)  
2 2p<sub>1/2</sub>, respectively [38,39]. Additionally, two relatively weak peaks resulting from  
3 shaking properties were observed for Cu(0) 2p<sub>3/2</sub> and Cu 2p<sub>1/2</sub> around 931.76 and 953.85  
4 eV, respectively. These peaks, attributable to Cu<sup>2+</sup>, are compelling evidence and indicate  
5 the presence of an 3d<sup>9</sup> open shell. The observation of Cu<sup>2+</sup> in the XPS spectrum can be  
6 explained as that Cu(0) NCats can be oxidized (CuO) due to exposure to air during sample  
7 preparation. [40,41]. The peak around 942.31 eV observed in Figure 2b was also  
8 attributed to the Cu<sup>2+</sup> satellite [42].

9 TEM images, histogram and EDX data of Cu(0) NCats were shown in Figure 3.  
10 TEM images were used to determine the morphology and calculate the average particle  
11 size of Cu(0) NCats. TEM images recorded in different magnifications (Figure 3a,b) and  
12 histogram (Figure 3c) showed that 266 non-touching Cu(0) NCats in-situ achieved using  
13 precursor Cu(acac)<sub>2</sub> throughout the green dehydrogenation of DMAB are well  
14 distributed. The average particle size of the Cu(0) NCats obtained in situ was calculated  
15 to be 2.9 ± 0.2 nm by single counting from the TEM image (Figure 3c). The particle size  
16 of Cu(0) NCats is comparable to other catalysts and it can be clearly seen that it is smaller  
17 than that of most other catalysts (see Table 1). As can be seen from the EDX data (Figure  
18 3d), the nanocatalyst sample contains an only copper element. Thus it can be said that our  
19 Cu(0) NCats are not oxidized during TEM sampling (see Section 2.2., The TEM grid also  
20 contains Cu) [26,27].

21 Figure 4 shows the powder XRD pattern and HR-TEM analysis of Cu(0) NCats  
22 synthesized in situ during the green dehydrogenation of DMAB. In the powder XRD  
23 pattern, it was observed that three reflection peaks were centered at 2θ = ~36.58, 43.28,  
24 50.42° and these peaks were assigned to Cu (111), (200) and (220) planes, indicating a

1 face-centered cubic structure in the crystal lattice (Figure 4a) [43,44]. The Cu(111)  
2 diffraction peak of the obtained nanocatalyst was used to calculate the average crystallite  
3 size and lattice parameter value of the metal nanocatalysts. Also, the Scherrer formula  
4 was used to calculate the average crystallite size of Cu(0) NCats and its size was  
5 calculated to be 2.78 nm. It can be clearly seen that this diameter is pretty close to the  
6 diameter (2.9 nm) calculated using the TEM image. HR-TEM analysis was used to  
7 investigate the crystallinity of the Cu(0) NCats synthesized in-situ during the green  
8 dehydrogenation of DMAB (Figure 4b). Accordingly, no agglomeration was observed for  
9 the Cu(0) NCats that were well distributed in hexane. As can be seen from Figure 4b, the  
10 plane of Cu(111) on the prepared nanocatalysts has an interval distance of 0.210 nm and  
11 is exceedingly close to the Cu(111) interval distance of 0.209 nm, and this finding is in  
12 agreement with the literature [25,45,46,47].

13 The product obtained after catalytic dehydrogenation of DMAB was properly  
14 characterized by  $^{11}\text{B}\{-^1\text{H}\}$ -NMR and ATR-FTIR spectroscopies (Figure 5).  $^{11}\text{B}\{-^1\text{H}\}$ -  
15 NMR spectra were recorded after preparation as described in Section 2.2 and used to  
16 determine the product obtained after the dehydrogenation reaction of DMAB (bottom)  
17 and pure DMAB (top). As shown in Figure 5a, the resonance signal of DMAB at  $\delta = -$   
18 14.58 ppm was replaced by the signal at  $\delta = 4.61$  ppm of the  $[\text{Me}_2\text{NBH}_2]_2$  (cyclic dimer)  
19 after the green dehydrogenation reaction. Also, ATR-FTIR spectra (Figure 5b) were used  
20 to show differences between pure DMAB and the product formed after the  
21 dehydrogenation reaction. According to this, the typical N-H bending and N-H stretching  
22 absorption bands of pure DMAB disappeared at 1155 and 3210  $\text{cm}^{-1}$ , respectively, while  
23 its B-H stretching bands at 2377 and 2271  $\text{cm}^{-1}$  were shifted to 1960  $\text{cm}^{-1}$  at the end of  
24 the dehydrogenation reaction [48]. Furthermore, the newly formed B-N stretching band

1 at 1615  $\text{cm}^{-1}$  in the FTIR spectrum of the  $[\text{Me}_2\text{NBH}_2]_2$  can be explained as a change in  
2 DMAB after the dehydrogenation reaction. All these data in the ATR-FTIR and  $^{11}\text{B}$ -  
3  $\{^1\text{H}\}$ -NMR spectra show that  $\text{Me}_2\text{NHBH}_3$  is fully transformed to the  $[\text{Me}_2\text{NBH}_2]_2$ .

### 4 **3.2. Calculation of activation energy from kinetic studies performed for green** 5 **dehydrogenation of DMAB catalyzed by Cu(0) NCats**

6 The kinetic study of the Cu(0) NCats formed in situ during the dehydrogenation of  
7 DMAB was carried out in three sets by observing the dihydrogen release as a function of  
8 catalyst and substrate amounts and reaction temperature.

9 In 1<sup>st</sup> set, while the reaction temperature and the amount of DMAB were fixed at  
10 nRT ( $30.0 \pm 0.1^\circ\text{C}$ ) and 2.0 mmol, respectively, the effect of catalyst amount on the  
11 dihydrogen release rate in the dehydrogenation of DMAB was investigated by varying  
12 the initial amount of copper in the range of  $[\text{Cu}]_0 = 0.10\text{-}0.30$  mmol (Figure 6). Figure 6a  
13 indicates the plots of time versus mol of hydrogen per mol of DMAB throughout  
14 dehydrogenation of DMAB, which was performed starting from a constant substrate  
15 amount of 2.0 mmol and various amounts of  $\text{Cu}(\text{acac})_2$  at nRT. An induction period ( $\sim 45$   
16 min) observed during the green dehydrogenation of DMAB can be explained as the time  
17 required for the formation the catalytically active copper nanocatalysts after the reduction  
18 of  $\text{Cu}(\text{acac})_2$ . As expected, the slope calculated from the linear part of the plots showed  
19 that there is a linear relationship between the dihydrogen release rate and the amount of  
20  $\text{Cu}(\text{acac})_2$  after the induction time. Figure 6b demonstrates the plot of the logarithmic  
21 initial rate of dihydrogen release, calculated from the slope of the plots in Figure 6a,  
22 versus the logarithmic initial amount of copper after induction period. The slope resulting  
23 from a linear fit of the plot is nearly 0.82, indicating that the dehydrogenation of DMAB  
24 is first-order with respect to the amount of  $\text{Cu}(\text{acac})_2$ .

1           In the 2<sup>nd</sup> set, the relationship between initial dihydrogen release rate and substrate  
2 amount was investigated by varying the initial amount of DMAB ( $[\text{DMAB}]_0 = 1.0\text{-}3.0$   
3 mmol) at constant copper amount (0.2 mmol) and temperature (nRT) (Figure 7). As  
4 shown in Figure 7a, the dihydrogen volume increased with the increasing amount of  
5 DMAB, but the induction period decreased throughout the dehydrogenation of DMAB.  
6 Plotting the logarithmic initial dihydrogen release rate versus the logarithmic initial  
7 DMAB amount in Figure 7b gives a straight line with a slope of about 0.34. This  
8 demonstrates that the dehydrogenation of DMAB is about half-order respect to the  
9 DMAB amount. In view of these results, the catalytic rate law for the dehydrogenation of  
10 DMAB catalyzed by Cu(0) NCats can be written as in Eq 2.

$$11 \quad \text{Rate} = k_{\text{app}}[\text{Cu}]^{0.82}[\text{DMAB}]^{0.34} \quad \text{Eq 2}$$

12           In the 3<sup>rd</sup> set, the effect of reaction temperature on the initial rate of dihydrogen  
13 release was examined at different temperatures in the range of 25-45°C, while amounts  
14 of DMAB and Cu(acac)<sub>2</sub> were kept constant at 2.0 and 0.2 mmol, respectively (Figure 8).  
15 As clearly shown in Figure 8a, the catalytic activity increased with increasing  
16 temperature, while the induction period decreased throughout the dehydrogenation of  
17 DMAB. The  $k_{\text{obs}}$  (observed rate constant) were calculated from the slopes of the  
18 dihydrogen release plots after the induction period and these values were used to  
19 determine the activation energy for the green dehydrogenation of DMAB using the  
20 Arrhenius plot in Figure 8b. The activation energy for the catalytic dehydrogenation of  
21 DMAB catalyzed by Cu(0) NCats was calculated from the Arrhenius plot as  $E_a = 16.6 \pm$   
22  $2 \text{ kJmol}^{-1}$ . Table 1 demonstrates that this activation energy may be the lowest activation  
23 energy achieved in the green dehydrogenation of DMAB performed using other catalysts.

### 24 **3.3. Lifetime study of Cu(0) NCats in the green dehydrogenation of DMAB**

1 The lifetime study of the copper catalyst was started by adding 2.0 mmol of DMAB to  
2 Cu(0) NCats (0.2 mmol) throughout the green dehydrogenation reaction at nRT. When  
3 dihydrogen release was complete, additional DMAB was added. This process was  
4 continued until no more hydrogen was released. As expected, the induction period  
5 observed with the first DMAB addition was not observed with the other additions. As a  
6 result of this experiment, TON and  $\text{TOF}_{\text{app}}$  were found to be 456.5 over 50 h and  $47.7 \text{ h}^{-1}$ ,  
7 respectively, during the green dehydrogenation of DMAB until deactivation of the  
8 copper catalyst because of bulk metal aggregation (Figure 9). TON and TOF values  
9 showed that Cu(0) NCats are highly stable and long-lived catalyst in the green  
10 dehydrogenation of DMAB, although no stabilizer or supporter was used. These  $\text{TOF}_{\text{app}}$   
11 and TON values can be compared with most other catalysts synthesized by both green  
12 (solvent-free) and conventional (in solvent) methods reported hitherto (Table 1). As can  
13 be seen in Table 1, the TOF value generally increases as the particle size of the metal  
14 catalysts decreases. The reason for this can be considered that the TON and the TOF  
15 values also increase, because the small particle size of the metal catalysts has large active  
16 surface areas.

### 17 **3.4. Heterogeneity Testing for Cu(0) NCats in the green dehydrogenation of DMAB**

18 To determine heterogeneity, a series of poisoning studies were performed for Cu(0)  
19 NCats in the green dehydrogenation of DMAB using  $\text{CS}_2$  as a poison, as detailed in  
20 Section 2.5 [49]. The use of  $\text{CS}_2$  is aimed to prevent the substrate from access the active  
21 site as a result of the strong binding of the poison to the metal center. Briefly, poisoning  
22 experiments for the green dehydrogenation of 2.0 mmol DMAB catalyzed by 0.2 mmol  
23 Cu(0) NCats were performed by adding 0.1 mol of  $\text{CS}_2$  per mol of copper under an inert  
24 atmosphere after 50% conversion of the green dehydrogenation of DMAB at nRT and



1 then monitoring the reaction by changes in dihydrogen pressure as in previous  
2 experiments. Figure 10 reveals that Cu(0) NCats were poisoned with a strong poison such  
3 as CS<sub>2</sub> and the dihydrogen release was fully halted after the addition of 0.1 equiv CS<sub>2</sub> to  
4 the reaction medium. This is the clearest indication that the catalysis is heterogeneous  
5 [50]. From these results, it can be concluded that the dehydrogenation of DMAB is a  
6 heterogeneous catalysis and Cu(0) NCats are the kinetically competent catalyst.

### 7 **3.5. Reusability and isolability of Cu(0) NCats in the green dehydrogenation of** 8 **DMAB**

9 Reusability and isolability are two crucial criteria for heterogeneous catalysts. Therefore,  
10 the reusability and isolability of Cu(0) NCats were tested for the green dehydrogenation  
11 of DMAB at nRT. When dehydrogenation of DMAB catalyzed by Cu(0) NCats in the 1<sup>st</sup>  
12 run was ceased, black powder of Cu(0) NCats was isolated and then washed with 3x20  
13 mL ethanol. The washed Cu(0) NCats was dried in vacuo and stored under inert  
14 atmosphere and this process was repeated 5 times. It was found that the initial activity  
15 and conversion at the 5<sup>th</sup> run of Cu(0) NCats in the dehydrogenation of DMAB were 81%  
16 and >99%, respectively (Figure 11a). Also, the dihydrogen release achieved to 1.0 equiv.  
17 in the whole catalytic runs. The catalytic activity of Cu(0) NCats decreased by 19% in the  
18 5th run. The increasing size of Cu(0) NCats because of the decrease in the number of  
19 atoms on the active surface and agglomeration of the metal can be shown to be the reason.  
20 TEM image (Figure 11b) and particle size histogram (Figure 11c) of Cu(0) NCats taken  
21 after the 5th use confirmed this condition, with the average size increasing from  $2.9 \pm 0.2$   
22 nm to  $5.3 \pm 0.2$  nm. Besides, poor mixing in the green environment might also have  
23 contributed negatively to the size growth of the metal. From these results, it was clear

1 understood that Cu(0) NCats exhibited quite high reusability and isolability in the green  
2 dehydrogenation of DMAB.

### 3 **4. Conclusions**

4 Consequently, in this work, an active, cheap and readily available metal such as copper  
5 was used as a catalyst for the green dehydrogenation of DMAB at nRT. It was found that  
6 the green dehydrogenation of DMAB catalyzed by Cu(0) NCats exhibited very high  
7 catalytic activity, although an induction time (~45 min) was observed during the in situ  
8 formation of Cu(0) NCats after Cu(acac)<sub>2</sub> reduction. Furthermore, the experiment of  
9 catalytic lifetime indicated that Cu(0) NCats was the long-lived catalyst with TON and  
10 TOF<sub>app</sub> values of 456.5 over 50 h and 47.7 h<sup>-1</sup>, respectively, before deactivation in the  
11 green dehydrogenation of DMAB at nRT. As understood from the reusability and  
12 isolability studies, Cu(0) NCats was easily distributed in hexane and its activity in the  
13 green dehydrogenation of DMAB did not change even after the 5<sup>th</sup> use. Also, its initial  
14 catalytic activity was retained by 81% even at the 5<sup>th</sup> run, while fully transformation of  
15 Me<sub>2</sub>NHBH<sub>3</sub> to [Me<sub>2</sub>NBH]<sub>2</sub> plus 1.0 equiv of dihydrogen was completed at nRT. On that  
16 account, this Cu(0) NCats having highly reusability and isolability is a good example for  
17 the green dehydrogenation of DMAB. **The novel and remarkable contribution of this**  
18 **study to the literature is that no stabilizers, solvents or supporters were used for the green**  
19 **dehydrogenation of DMAB in nRT. Moreover, the characterization of heterogeneous**  
20 **Cu(0) NCats has been reported to be very economical with this new method using**  
21 **advanced spectroscopic techniques.** It was observed that Cu(0) NCats with particle size  
22 of 2.9±0.2 nm exhibited rather high activity in green dehydrogenation of DMAB. Kinetic  
23 studies on 1<sup>st</sup> and 2<sup>nd</sup> sets showed that the green dehydrogenation of DMAB catalyzed by  
24 Cu(0) NCats is first-order with respect to catalyst amount, while it is about half-order

1 with respect to DMAB amount. Also, the kinetic study on 3<sup>rd</sup> set reveals that examination  
2 of temperature change is of great importance for calculation of the activation energy for  
3 dihydrogen release rate in the green dehydrogenation of DMAB catalyzed by Cu(0)  
4 NCats. As can be clearly seen in Table 1, the activation energy for the green  
5 dehydrogenation of DMAB catalyzed by Cu(0) NCats ( $E_a = 16.6 \pm 2 \text{ kJ mol}^{-1}$ ) in the green  
6 medium at nRT is much lower than achieved by using both Ni(0) nanoparticles ( $E_a = 42$   
7  $\pm 2 \text{ kJ mol}^{-1}$ ) at  $25.0 \pm 0.1^\circ\text{C}$  [26] and Ru NCs ( $E_a = 18 \pm 2, 45 \pm 2, 25 \pm 2 \text{ kJ mol}^{-1}$  for  
8 Ru@PVP, Ru@PS-co-MA and Ru@Al<sub>2</sub>O<sub>3</sub> NCs, respectively) at  $35.0 \pm 0.1^\circ\text{C}$  [27]. The  
9 orders of activation energies for the above catalysts obtained for the similar reactions are  
10 lined up as Cu(0) nanocatalysts < Ru@PVP NCs  $\approx$  Ru@Al<sub>2</sub>O<sub>3</sub> nanoclusters < Ni(0)  
11 nanoparticles < Ru@PS-co-MA nanoclusters.

12 **The very economical preparation of Cu(0) NCats in solvent-free media shows that**  
13 **it is an environmentally friendly and atom-economical catalyst in hydrogen production.**  
14 **It can be clearly stated that this method will open a new path for the design of transition**  
15 **metal catalysts with good dispersibility and high stability in the future and provide**  
16 **alternative catalysts.**

### 17 **Acknowledgements**

18 This work was supported as financial by Bingol University Scientific Research Projects  
19 (BUBAP, Project Number: BAP-130-97-2011).

## 1 References

---

- [1] Graetz J. New approaches to hydrogen storage. *Chemical Society Reviews* 2009; 38 (1): 73–82. doi:10.1039/B718842K
- [2] Staubitz A, Robertson APM., Manners I. Ammonia-borane and related compounds as dihydrogen sources. *Chemical Reviews* 2010; 110 (7): 4079–4124. doi:10.1021/cr100088b
- [3] United States. Dept. of Energy. Office of Science. Basic research needs for the hydrogen economy. report of the basic energy sciences workshop on hydrogen production, storage and use. May 13-15, 2003. doi:10.2172/899224
- [4] EIA, Annual Energy Outlook, U.S. Energy Inf. Adm., ES-5; 2016. doi:EIA-0383
- [5] IAC, Lighting the way Toward a sustainable energy future, Interacademy Council. 2007; 31.
- [6] Acidereli H, Cellat K, Calimli MH, Sen F. Palladium/ruthenium supported on graphene oxide (PdRu@GO) as an efficient, stable and rapid catalyst for hydrogen production from DMAB under room conditions. *Renewable Energy* 2020; 161: 200-206. doi:10.1016/j.renene.2020.07.105
- [7] Feng W, Yang L, Cao N, Du C, Dai H et al. In situ facile synthesis of bimetallic CoNi catalyst supported on graphene for hydrolytic dehydrogenation of amine borane. *International Journal of Hydrogen Energy* 2014; 39 (7): 3371-3380. doi:10.1016/j.ijhydene.2013.12.113
- [8] Staubitz A, Robertson APM, Sloan ME, Manners I. Amine and phosphine borane adducts: New interest in old molecules. *Chemical Reviews* 2010; 110 (7): 4023–4078. doi:10.1021/cr100105a

- 
- [9] Van den Berg AWC, Areán CO. Materials for hydrogen storage: Current research trends and perspectives. *Chemical Communications* 2008; (6): 668–681. doi:10.1039/b712576n
- [10] Kundu D, Pugazhenti G, Banerjee T. Low- to room-temperature dehydrogenation of dimethylamine borane facilitated by ionic liquids: molecular modeling and experimental studies. *Energy Fuels* 2020; 34 (10): 13167–13178. doi:10.1021/acs.energyfuels.0c01896
- [11] Jaska CA, Temple K, Lough AJ, Manners I. Catalytic dehydrocoupling of amine-borane adducts to form aminoboranes and borazines. *Phosphorus, Sulfur Silicon Related Elements* 2004; 179 (4-5): 733–736. doi:10.1080/10426500490426683
- [12] Turner J, Sverdrup G, Mann MK, Maness P, Kroposki B, Ghirardi M, Evans RJ, Blake D. Renewable hydrogen production. *International Journal of Energy Research* 2008; 32 (5): 379–407. doi:10.1002/er.1372
- [13] Karaboga S, Ozkar S. Nanoalumina supported palladium(0) nanoparticle catalyst for releasing H<sub>2</sub> from dimethylamine borane. *Applied Surface Science* 2019; 487: 433-441. doi:10.1016/j.apsusc.2019.05.087
- [14] Zahmakiran M, Özkar S. Dimethylammonium hexanoate stabilized rhodium(0) nanoclusters identified as true heterogeneous catalysts with the highest observed activity in the dehydrogenation of dimethylamine-borane. *Inorganic Chemistry* 2009; 48 (18): 8955–8964. doi:10.1021/ic9014306
- [15] Yempally V, Moncho S, Wang YY, Kyran SJ, Fan WY et al. Thermal dehydrogenation of dimethylamine borane catalyzed by a bifunctional rhenium complex. *Organometallics* 2019; 38 (13): 2602-2609. doi:10.1021/acs.organomet.9b00115

- 
- [16] Zahmakıran M, Tristany M, Philippot K, Fajerweg K, Özkar S, Chaudret B. Aminopropyltriethoxysilane stabilized ruthenium(0) nanoclusters as an isolable and reusable heterogeneous catalyst for the dehydrogenation of dimethylamine–borane. *Chemical Communications* 2010; 46 (17): 2938–2940. doi:10.1039/c000419g
- [17] Beweries T, Hansen S, Kessler M, Klahn M, Rosenthal U. Catalytic dehydrogenation of dimethylamine borane by group 4 metallocene alkyne complexes and homoleptic amido compounds. *Dalton Transactions* 2011; 40 (30): 7689–7692. doi:10.1039/c1dt10366k
- [18] Kalidindi SB, Esken D, Fischer RA. B-N Chemistry@ZIF-8: Dehydrocoupling of dimethylamine borane at room temperature by size-confinement effects. *Chemistry—A European Journal* 2011; 17 (24): 6594–6597. doi:10.1002/chem.201100518
- [19] Sen B, Kuyuldar E, Savk A, Calimli, H, Duman S et al. Monodisperse ruthenium-copper alloy nanoparticles decorated on reduced graphene oxide for dehydrogenation of DMAB. *International Journal of Hydrogen Energy* 2019; 44 (21): 10744-10751. doi:10.1016/j.ijhydene.2019.02.176
- [20] Tang CY, Phillips N, Bates JI, Thompson AL, Gutmann MJ, Aldridge S. Dimethylamine borane dehydrogenation chemistry: syntheses, X-ray and neutron diffraction studies of 18-electron aminoborane and 14-electron aminoboryl complexes. *Chemical Communications* 2012; 48 (65): 8096–8098. doi:10.1039/c2cc33361a
- [21] Duman S, Özkar S. Oleylamine-stabilized ruthenium(0) nanoparticles catalyst in dehydrogenation of dimethylamine-borane. *International Journal of Hydrogen Energy* 2013; 38 (24): 10000–10011. doi:10.1016/j.ijhydene.2013.05.119
- [22] Cui P, Spaniol TP, Maron L, Okuda J. Dehydrogenation of amine-borane  $\text{Me}_2\text{NH}\cdot\text{BH}_3$  catalyzed by a lanthanum-hydride complex. *Chemistry—A European*

---

Journal 2013; 19 (40): 13437–13444. doi:10.1002/chem.201301732

[23] Zhu JW, Zins EL, Alikhani ME. Dehydrocoupling of dimethylamine borane by titanocene: Elucidation of ten years of inconsistency between theoretical and experimental descriptions. *Physical Chemistry Chemical Physics* 2018; 20 (23): 15687-15695. doi:10.1039/c8cp01970c

[24] Pal S, Kusumoto S, Nozaki K. Dehydrogenation of dimethylamine-borane catalyzed by half-sandwich Ir and Rh complexes: Mechanism and the role of Cp\* noninnocence. *Organometallics* 2018; 37 (6): 906-914. doi:10.1021/acs.organomet.7b00889

[25] Duman S, Özkar S. Oleylamine-Stabilized Copper(0) Nanoparticles: An Efficient and Low-Cost Catalyst for the Dehydrogenation of Dimethylamine Borane. *ChemCatChem* 2017; 9 (13): 2588–2598. doi:10.1002/cctc.201700367

[26] Demir H, Duman S. Monodisperse nickel nanoparticles in the solvent-free dehydrogenation of dimethylamine borane. *International Journal of Hydrogen Energy* 2015; 40 (32): 10063–10071. doi:10.1016/j.ijhydene.2015.06.093

[27] Bukan B, Duman S. Green dehydrogenation of dimethylamine-borane catalyzed by in situ generated ruthenium nanoclusters in presence of various supporters and its comparison with classical methods. *International Journal of Hydrogen Energy* 2018; 43 (17): 8278–8289. doi:10.1016/j.ijhydene.2018.03.072

[28] Nako AE, White AJP, Crimmin MR. Bis( $\sigma$ -B-H) complexes of copper(i): precursors to a heterogeneous amine-borane dehydrogenation catalyst. *Dalton Transactions* 2015; (44): 12530–12534. doi:10.1039/c5dt02144h

[29] Sanyal U, Jagirdar BR. Metal and alloy nanoparticles by amine-borane reduction of metal salts by solid-phase synthesis: Atom economy and green process. *Inorganic Chemistry* 2012; 51 (23): 13023–13033. doi:10.1021/ic3021436

- 
- [30] Gülcan M, Zahmakiran M, Özkar S. Palladium(0) nanoparticles supported on metal organic framework as highly active and reusable nanocatalyst in dehydrogenation of dimethylamine-borane. *Applied Catalysis B: Environmental* 2014; 147: 394–401. doi:10.1016/j.apcatb.2013.09.007
- [31] Yurderi M, Bulut A, Zahmakiran M, Gülcan M, Özkar S. Ruthenium(0) nanoparticles stabilized by metal-organic framework (ZIF-8): Highly efficient catalyst for the dehydrogenation of dimethylamine-borane and transfer hydrogenation of unsaturated hydrocarbons using dimethylamine-borane as hydrogen source. *Applied Catalysis B: Environmental* 2014; 160–161: 534–541. doi:10.1016/j.apcatb.2014.06.009
- [32] Barin EÜ, Masjedi M, Özkar S. A new homogeneous catalyst for the dehydrogenation of dimethylamine borane starting with ruthenium(III) acetylacetonate. *Materials (Basel)* 2015; 8 (6): 3155–3167. doi:10.3390/ma8063155
- [33] Duman S, Masjedi M, Özkar S. Highly active and long lived homogeneous catalyst for the dehydrogenation of dimethylamine borane starting with ruthenium(III) acetylacetonate and oleylamine precatalyst. *Journal of Molecular Catalysis A: Chemical* 2016; 411: 9-18. doi:10.1016/j.molcata.2015.08.006
- [34] Çelik B, Kuzu S, Erken E, Sert H, Koşkun Y, Şen F. Nearly monodisperse carbon nanotube furnished nanocatalysts as highly efficient and reusable catalyst for dehydrocoupling of DMAB and C1 to C3 alcohol oxidation. *International Journal of Hydrogen Energy* 2016; 41 (4): 3093–3101. doi:10.1016/j.ijhydene.2015.12.138
- [35] Laidler K. *Chemical Kinetics*. Harper Row 1987; 1: 233–270. doi:10.1007/0-306-48390-4\_2
- [36] Yodaa S, Takebayashia Y, Suea K, Furuyaa T, Otake K. Thermal decomposition of copper (II) acetylacetonate in supercritical carbon dioxide: In situ observation via UV–vis



---

spectroscopy. *The Journal of Supercritical Fluids* 2017; 123 82–91.

doi:10.1016/j.supflu.2016.12.017

[37] Creighton JA, Eadon DG. Ultraviolet–visible absorption spectra of the colloidal metallic elements. *Journal of the Chemical Society, Faraday Transactions* 1991; 87 (24): 3881–3891. doi:10.1039/FT9918703881

[38] Tanyıldızı S, Morkan İ, Özkar S. Ceria supported copper(0) nanoparticles as efficient and cost-effective catalyst for the dehydrogenation of dimethylamine borane. *Molecular Catalysis* 2017; 434: 57–68. doi:10.1016/j.mcat.2017.03.002

[39] Miller AC, Simmons GW. Copper by XPS. *Surface Science Spectra* 1993; 2: 55–56. doi:10.1116/1.1247725

[40] Wu JCS, Tseng IH, Chang WC. Synthesis of titania-supported copper nanoparticles via refined alkoxide sol-gel process. *Journal of Nanoparticle Research* 2001; 3: 113–118. doi:10.1023/A:1017553125829

[41] Chusuei CC, Brookshier MA, Goodman DW. Correlation of relative X-ray photoelectron spectroscopy shake-up intensity with CuO particle size. *Langmuir* 1999; 15 (8): 2806–2808. doi:10.1021/la9815446

[42] Xu D, Fan D, Shen W. Catalyst-free direct vapor-phase growth of Zn<sub>1-x</sub>Cu<sub>x</sub>O micro-cross structures and their optical properties. *Nanoscale Research Letters* 2013; 8 (1): 46. doi:10.1186/1556-276X-8-46

[43] Wallace PL, Weissmanna S, Mueller MH, Calveit LD, Jenkins R. The new ICDD Metals and Alloys Indexes: Usefulness and potentialities. *Powder Diffraction* 1994; 9 (4): 239-245. doi:10.1017/S0885715600018947

- 
- [44] McMurdie HF, Morris MC, Evans EH, Paretzkin B, Wong-Ng W, Ettliger L, Hubbard CR. Standard X-Ray Diffraction Powder Patterns from the JCPDS Research Associateship. *Powder Diffraction* 2013; 1 (2): 64-77. doi: 10.1017/S0885715600011593
- [45] Gao W, Zhao Y, Liu J, Huang Q, He S, Li C, Zhao J, Wei M. Catalytic conversion of syngas to mixed alcohols over CuFe-based catalysts derived from layered double hydroxides. *Catalysis Science & Technology* 2013; 3 (5): 1324–1332. doi:10.1039/C3CY00025G
- [46] Barrabes N, Cornado D, Foettinger K, Dafinov A, Llorca J, Medina F, Rupprechter G. Hydrodechlorination of trichloroethylene on noble metal promoted Cu-hydrotalcite-derived catalysts. *Journal of catalysis* 2009; 263 (2): 239–246. doi:10.1016/j.jcat.2009.02.015
- [47] Gao W, Zhao Y, Chen H, Chen H, Li Y, He S, Zhang Y, Wei M, Evans DG, Duan X. Core-shell Cu@(CuCo-alloy)/Al<sub>2</sub>O<sub>3</sub> catalysts for the synthesis of higher alcohols from syngas. *Green Chemistry* 2015; 17 (3): 1525–1534. doi:10.1039/c4gc01633e
- [48] Friedrich A, Drees M, Schneider S. Ruthenium-catalyzed dimethylamine borane dehydrogenation: Stepwise metal-centered dehydrocyclization. *Chemistry—A European Journal* 2009; 15 (40): 10339–10342. doi:10.1002/chem.200901372
- [49] Widegren JA, Finke RG. A review of the problem of distinguishing true homogeneous catalysis from soluble or other metal-particle heterogeneous catalysis under reducing conditions. *Journal of Molecular Catalysis A: Chemical* 2003; 198 (1-2): 317–341. doi:10.1016/S1381-1169(02)00728-8
- [50] Lin Y, Finke RG. A More General Approach to Distinguishing “Homogeneous” from “Heterogeneous” Catalysis: Discovery of Polyoxoanion- and Bu<sub>4</sub>N<sup>+</sup>-Stabilized,

---

Isolable and Redissolvable, High-Reactivity Ir.apprx.190-450 Nanocluster Catalysts.

Inorganic Chemistry 1994; 33 (22): 4891–4910. doi:10.1021/ic00100a012